Environmental Science Processes & Impacts

ROYAL SOCIETY OF CHEMISTRY

PAPER

View Article Online
View Journal

Cite this: DOI: 10.1039/d1em00056j

# Could chemical exposure and bioconcentration in fish be affected by slow binding kinetics in blood?†

Sophia Krause *[a] and Kai-Uwe Goss [ab]

Received 1st February 2021
Accepted 26th March 2021

DOI: 10.1039/d1em00056j

rsc.li/espi

The possible implications of slow binding kinetics on respiratory uptake, bioconcentration and exposure of chemicals were evaluated in the present study. Most physiological and chemical information needed for such an evaluation is already known from the literature or can be estimated. However, data for binding kinetics of chemicals in fish plasma have not been reported in the literature yet. In the first part of this study, we therefore experimentally investigated the plasma binding kinetics for ten chemicals, including pollutants like polycyclic aromatic hydrocarbons and a pesticide. The determined desorption rate constants were in the range of 0.4 $s^{-1}$ to 0.1 $s^{-1}$. In the second part of this study, we present a comparative modeling analysis of generic predictions with binding kinetics of different velocities. For doing so, a model that explicitly represents binding kinetics in blood was developed and applied for different hypothetical scenarios. The evaluation showed that slow sorption kinetics only limits respiratory uptake and thus influences the levels of bioaccumulation for extreme and, by that, rather unlikely parameter combinations (*i.e.* for strongly sorbing chemicals with very slow binding kinetics). It can therefore be assumed that limitations on respiratory uptake due to slow binding kinetics in blood are rather unlikely for most chemicals.

### Environmental significance

Predicting bioaccumulation or exposure in fish is increasingly becoming a promising alternative to animal testing. In this study, we investigate the impact of binding kinetics in blood on branchial uptake in fish because accurate representation of uptake is essential for such predictions. Slow binding kinetics in gill blood could result in the blood not being able to fully utilize its transport capacity for the chemical, resulting in less chemical reaching the periphery of the organism. We experimentally determined rate constants for plasma binding kinetics for a set of chemicals and developed a mathematical model for evaluation of the impact of binding kinetics. The analysis shows that limiting effects due to slow binding kinetics appear unlikely for most chemicals.

## Introduction

The use of predictive models for screening or assessment of chemicals regarding their bioaccumulation potential is regarded as a promising approach to reduce the use of animal testing. Particularly the prediction of bioconcentration factors (BCFs) has recently been subject of various studies[1–5] because the BCF is an accepted regulatory criterion. One important aspect for the predictive performance of such models is the consideration of elimination *via* biotransformation. For obtaining reliable estimates of biotransformation kinetics, so-called *in vitro* biotransformation assays were developed and refined in recent years, and finally two OECD test guidelines on this topic have been published.[6,7] The so determined *in vitro* rate constants are then mathematically converted into corresponding *in vivo* rate constants that can be used in BCF prediction models. Another important aspect for an accurate prediction of BCFs is the appropriate representation of chemical uptake. The importance of accurate uptake estimates has led to the development of plenty of methods for estimating uptake rate constants. A comprehensive overview of existing methods for estimation of respiratory uptake rate constants is provided by Brooke *et al.*[8] In their study, Brooke *et al.* concluded that it is difficult to recommend one specific method for prediction of respiratory uptake because several methods showed similar performance. However, even the "best" performing methods showed notable uncertainty (standard deviations of about 0.5 log-units), making the estimation of respiratory uptake a major source of uncertainty in BCF prediction. In general, the respiratory uptake rate depends on ventilation, permeation of the chemical into gill blood and the capacity of the gill blood to transport the chemical into the body. When present in blood, most of the chemicals tend to bind to blood components like proteins and lipids; especially for hydrophobic chemicals where

[a]Helmholtz Centre for Environmental Research, Department of Analytical Environmental Chemistry, Permoserstr. 15, 04318 Leipzig, Germany. E-mail: sophia.krause@ufz.de

[b]University of Halle-Wittenberg, Institute of Chemistry, Kurt-Mothes-Str. 2, 06120 Halle, Germany

† Electronic supplementary information (ESI) available. See DOI: 10.1039/d1em00056j

the freely dissolved chemical fraction in blood is usually small. Commonly, it is assumed that binding of the chemical to blood components is an instantaneous process. However, if the assumption of instantaneous binding was incorrect and sorption kinetics was slow, this could have consequences for the transport capacity of the blood and subsequent processes in the organism. Especially in the pharmaceutical literature, different experimental approaches have been developed for investigation of binding kinetics[9–12] and the topic has already gained much attention with a strong focus on potential implications of slow binding kinetics for drug elimination and distribution within the body.[13–18] In general, these studies demonstrate that, in most cases, binding kinetics is faster than the subsequent pharmacokinetic processes so that limitations of drug elimination or distribution due to slow binding kinetics can be regarded as unlikely. However, analogous to the potential effects on chemical elimination and distribution, slow binding kinetics could also affect chemical uptake. To our knowledge, this topic has not yet been systematically evaluated. In this study, we want to focus on potential effects of slow binding kinetics on respiratory uptake in fish. For the scenario of respiratory uptake in fish, slow binding kinetics in blood would mean that the blood could not exploit its full capacity to transport the chemical from the gills into the periphery and thus could not keep up a high chemical gradient between ventilated water and gill tissue. As a consequence, less chemical could be taken up into the gills and one would expect lower chemical concentrations in the organism compared to a scenario with instantaneous binding in blood. By this, slow binding kinetics could lead to lower levels of bioaccumulation in the organism. The question whether and to what extent these effects occur for realistic parameter combinations is what we want to discuss in this study.

For this purpose, we combine experimental data on binding kinetics in fish plasma with suitable modeling approaches to evaluate the implications of slow binding kinetics on respiratory uptake of chemicals in fish. To investigate how fast binding kinetics in plasma is, the desorption kinetics of a set of organic chemicals (including polycyclic aromatic hydrocarbons and substituted benzenes) was determined experimentally using a recently described method.[19] This method for experimental determination of desorption rate constants involves the time-resolved extraction of the test chemicals from rainbow trout plasma. The use of plasma instead of whole blood in the experiments is due to the better handling and with regard to partitioning, plasma is generally considered a suitable surrogate for whole blood.[20] However, we cannot completely exclude the possibility that kinetics of specific sorption processes to individual components of whole blood may differ from those to plasma components. Combination of the determined desorption rate constants with the corresponding equilibrium constants for plasma binding of the chemicals allows for derivation of the rate constants for the reverse process (*i.e.* for sorption to the plasma components). The derived kinetic information is then used to assess whether binding kinetics in plasma limits respiratory uptake of chemicals. For the quantitative evaluation of the impact of binding kinetics on respiratory uptake of chemicals, a model structure that incorporates binding kinetics in blood was developed and compared with a simpler model that assumes instantaneous binding equilibrium. We apply the model for different parameter combinations to gain a general mechanistic understanding of the influence of binding kinetics on chemical uptake and bioaccumulation.

For clarity, we want to start with some – often misinterpreted – theories and concepts that are frequently brought up in discussions on the exchange kinetics between blood and neighboring compartments. For example, the idea often arises that the bound fraction of a chemical could also be available for uptake into eliminating tissues or for uptake by degrading enzymes in contrast to the otherwise accepted paradigm that only the freely dissolved fraction of a chemical is relevant. Some authors thus insinuate that the actual available amount of chemical may be greater than conceptually represented in the models that refer to the unbound fraction.[21–23] In fact, however, theoretical considerations show that models which refer to freely dissolved chemical concentrations already reflect the availability of the bound fraction. If instantaneous sorption in blood is assumed, this conceptually means that free molecules removed from the blood are immediately replaced by molecules from the bound state. It does not matter whether one assumes that freely dissolved chemical is taken up or whether a direct uptake of bound chemical (*i.e.* without the chemical transitioning into the freely dissolved state) is also possible. By assuming instantaneous equilibrium between free and bound chemical, the underlying information is redundant. Thus, it is conceptually irrelevant whether one refers to the freely dissolved fraction when quantifying elimination (which is the typical approach) or whether one refers to the bound fraction. Thought through consistently, both approaches (no matter which reference is used) lead to the same result in the end. The only exception are models that assume the bound fraction to be irreversibly bound and, by this, not available for uptake under any circumstances.

Another reasoning suggests that protein facilitated transport of the bound chemical could enhance chemical uptake,[21,23,24] *e.g.* the uptake from blood into biotransforming tissues like the liver. Facilitated transport is therefore sometimes suggested as an explanation for why *in vitro*-based predictions underestimate *in vivo* biotransformation. Various studies have shown that the phenomenon of facilitated transport can indeed increase uptake or exchange rate of a chemical between two phases.[25–27] A prerequisite for this effect, however, is that the exchange of the freely dissolved chemical has been kinetically limited in the first place.[27,28] Exactly this point does not apply to the classical models of chemical elimination, such as those used *e.g.* for *in vitro–in vivo* extrapolation of hepatic biotransformation data. These models[3,29] make the simplifying assumption that the exchange of the chemical between blood and eliminating tissue is instantaneous. Facilitated transport as an explanation why these models underestimate hepatic elimination is thus not applicable, because no process can become faster than instantaneous.

 

Thus, on the subject of sorption in blood, arguments are sometimes put forward for observed discrepancies between model-based BCF predictions and *in vivo* measurements that are not consistent with the actual concepts/models applied.[20,30] The model applied here takes into account a kinetic limitation between bound and unbound chemical in blood, but does not represent any further kinetic limitation for the permeation of the chemical into surrounding tissues, such as slow membrane permeability. Consequently, free molecules removed from the blood are replaced by molecules from the bound state according to the prevailing kinetics but acceleration of chemical uptake from blood into tissues due to facilitated transport does not apply here, because this exchange process is *a priori* assumed to be instantaneous.

# Methods

### Experiments for determination of desorption kinetics

For determination of desorption kinetics, time-resolved extractions of the test chemicals (see Table 1) from diluted rainbow trout plasma were performed as described elsewhere.[19] In short, 200 μL of the plasma solution spiked with test chemical were pumped through a PDMS coated capillary with defined flow rates (24–0.2 mL $h^{-1}$) using a syringe pump (VIT-FIT syringe pump, Lambda Laboratory Instruments). Rainbow trout plasma was provided from the Toxicology Centre of the University of Saskatchewan and a protein content of 21.5 mg $mL^{-1}$ was given for undiluted plasma. Depending on the estimated partition behavior of the test chemicals (see ESI Section 1† for details on the estimation of the required partition coefficients), different dilution factors for the plasma were chosen to ensure (a) a high bound fraction of the chemical in the plasma solution and (b) a sufficient capacity of the PDMS for nearly complete extraction of the chemical from the plasma solution in the capillary. For each test chemical, the experiment was performed twice using differently diluted plasma solutions (used plasma dilutions for each chemical see ESI Section 1†). The purpose of this procedure is to confirm the determined rate constants because the kinetics should be independent from the used plasma concentration. For dilution of the plasma, Cortland's saline (124 mM NaCl, 5.1 mM KCl, 3.0 mM $NaH_2PO_4 \cdot H_2O$, 11.9 mM $NaHCO_3$, 0.94 mM $MgSO_4 \cdot 7H_2O$, 1.6 mM $CaCl_2 \cdot 2H_2O$, 10 mM HEPES, pH 7.8) was used. Stock solutions of the chemicals were prepared in methanol or in isopropanol and spiked into the diluted plasma (used chemical concentrations see ESI Section 1†). The solvent content in the final plasma solution did not exceed 0.5 v/v%. For equilibration, the spiked plasma solutions were incubated on a roller mixer over night at 11 °C.

The PDMS coated capillary used in the experiments was purchased from Quadrex Corporation (007-1, inner diameter 0.25 mm, layer 8 μm of 100% polydimethylsiloxane). A PDMS coated fiber (Polymicro Technologies Inc., diameter of the glass core 0.123 mm, layer 30 μm of 100% polydimethylsiloxane) was inserted into the capillary to further increase the PDMS sorption capacity and reduce the diffusion path lengths inside the capillary. Pieces of 20 cm length of capillary and fiber were used for the experiments. After passage through the capillary, the capillary effluent was collected and extracted under gentle shaking for 3 min with 1 mL cyclohexane for concentration determination. To compare the determined concentrations with the initial concentrations, samples of the original spiked plasma solution (not pumped through the capillary) were also extracted with cyclohexane in the same manner. Extraction efficiency for each chemical was calculated based on the chemicals' physico-chemical properties and was >99% for all test chemicals. The concentration determination was performed *via* GC-MS (7890A/5975C, Agilent Technologies, injection in cold splitless mode, separation with an HP-5MS column from Agilent Technologies).

### Data evaluation of the desorption experiments

The concentrations of the test chemical in the capillary effluent relative to the initial concentrations were plotted over the corresponding residence times inside the capillary to yield concentration–time-profiles. The desorption rate constants of the chemicals were determined from these concentration–time-profile *via* fitting a transport model that considers convection and dispersion as well as the partitioning kinetics between sorbing components of plasma and PDMS. For a detailed description of the transport model we refer to a recently published paper using the same experimental method and data analysis procedure for determining the desorption kinetics from albumin.[19] In order to adapt the transport model for the

Table 1 Summary of the determined desorption and sorption rate constant ($k_{des}$ and $k_{sorb}$) and the corresponding partition coefficients between sorbing plasma components and water ($K_{sorbcomp/w}$)

| Test chemical | log $K_{OW}$ [L $L^{-1}$] | $k_{des}$ [$s^{-1}$] | $k_{sorb}$ [$L_W$ $L_{sorbcomp}^{-1}$ $s^{-1}$] | log $K_{sorbcomp/w}$ fitted [L $L^{-1}$] |
|---|---|---|---|---|
| Phenanthrene | 4.4 | 0.3 | 1699 | 3.75 |
| *n*-Propylbenzene | 3.7 | 0.2 | 40 | 2.30 |
| 1,8-Dibromooctane | 4.8 | 0.2 | 1133 | 3.75 |
| 1,2,3,4-Tetrachlorobenzene | 4.6 | 0.4 | 1412 | 3.55 |
| Di-*n*-pentylether | 4.3 | 0.15 | 75 | 2.70 |
| *n*-Hexylbenzene | 5.3 | 0.1 | 600 | 3.78 |
| Chlorpyrifos | 5.2 | 0.1 | 400 | 3.60 |
| 1,4-Dibromobenzene | 3.8 | 0.3 | 165 | 2.74 |
| Pyrene | 4.6 | 0.15 | 1800 | 4.08 |
| 1,2,4-Trichlorobenzene | 4.1 | 0.2 | 80 | 2.60 |

here performed experiments with plasma, the albumin compartment of the original model[19] was replaced by a compartment, which represents the total of all sorbing plasma components. Thus, the heterogeneous individual components of the plasma (*e.g.* different proteins or lipoproteins) were combined to a single joint compartment. As mentioned above, the partitioning constants of the chemicals towards this compartment were estimated using the approach presented by Endo *et al.*[31] (see ESI Section 1†) and adjusted based on the generated concentration–time profiles. Adjustment of the partition coefficients based on the two generated concentration–time profiles for each chemical (differing in the used plasma dilution) is possible because the results for the shortest and longest residences inside the capillary are governed by the partition properties.[19] It is not surprising that these adjustments are necessary considering the fact that the data used to estimate the partition coefficients are not fish derived, *e.g.* for partitioning into the trout plasma proteins the partitioning to bovine albumin was used as surrogate.

### Modeling approaches for quantitative evaluation of the impact of binding kinetics

To investigate the influence of binding kinetics in gill blood on chemical uptake, two steady-state models are developed for a fish living under constant exposure to contaminated water but eating uncontaminated food. One model represents a scenario with binding kinetics in blood, the other model represents a scenario with instantaneous chemical equilibrium in blood between the bound state (at transport proteins or lipids) and the freely dissolved state and is illustrated in Fig. 1.

The model that considers binding kinetics in blood additionally distinguishes bound and freely dissolved chemical in the blood compartments; a detailed illustration of this model can be found in ESI Section 2b.† Both steady-state models represent uptake and elimination of the chemical *via* ventilation and transport of the chemical into the periphery of the organism with blood flow. Additionally, elimination of the chemical in the periphery, *e.g. via* fecal egestion or hepatic biotransformation, is also represented in both models. Both models rely on individual mass balances for the represented compartments (see ESI Section 2†). Both models are expressed as linear systems of equations and solved in MS Excel using matrix functions (MMULT, MINV) for steady state. As a result, the steady-state concentrations of the chemical in the ventilated water flowing out of the gills, in blood flowing out of the gills and into the gills and in the periphery of the fish are calculated.

For quantification of the impact of sorption kinetics, we use the resulting steady-state concentrations to calculate uptake efficiency ($E_{uptake}$), elimination efficiency ($E_{elimination}$) and bioconcentration factor (BCF) as a measure of bioaccumulation. The steady-state uptake efficiency $E_{uptake}$ describes to which extent a chemical is taken up from the respirated water and is calculated from the steady-state concentrations of the chemical in the respired water flowing into and out of the gills, $C_{W,in}$ and $C_{W,out}$:

$$E_{uptake} \equiv \frac{C_{W,in} - C_{W,out}}{C_{W,in}} \quad (1)$$

The steady-state elimination efficiency $E_{elimination}$ in contrast describes to which extent a chemical is removed from blood due to elimination in the periphery (*e.g. via* biotransformation). The elimination efficiencies for freely dissolved chemical and bound chemical in blood have to be calculated separately using the corresponding steady-state concentrations in blood ($C_{blood\text{-}free}$ and $C_{blood\text{-}bound}$) flowing into and out of the periphery.

$$E^{free}_{elimination} \equiv \frac{C_{blood\text{-}free,gills} - C_{blood\text{-}free,periphery}}{C_{blood\text{-}free,gills}} \quad (2)$$

$$E^{bound}_{elimination} \equiv \frac{C_{blood\text{-}bound,gills} - C_{blood\text{-}bound,periphery}}{C_{blood\text{-}bound,gills}} \quad (3)$$

These two elimination efficiencies can then be combined to yield the total elimination efficiency considering sorption kinetics in blood:

$$E^{total}_{elimination} = f_{unbound} \times E^{free}_{elimination} + f_{bound} \times E^{bound}_{elimination} \quad (4)$$

The BCF is calculated by combining the steady-state concentrations in the different body compartments ($C_{gills}$,

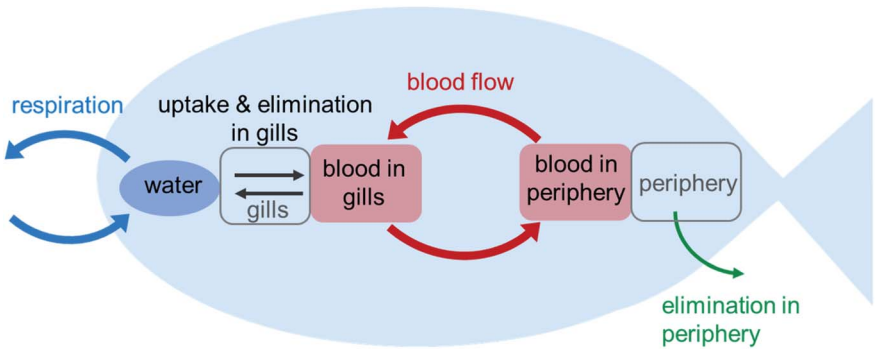


Fig. 1 Schematic overview of the modelled processes. Illustrated is the model that assumes instantaneous equilibrium in blood. Chemical uptake, elimination and exchange *via* blood flow are modelled as kinetic processes; instantaneous equilibrium between gills and gill blood and between periphery and peripheral blood is assumed.

 

$C_{periphery}$, $C_{blood,periphery}$, $C_{blood,gills}$) with the corresponding volume information to derive the steady-state whole-body concentration (see ESI Section 2† for details).

$$BCF = \frac{\left(C_{gills}V_{gills} + C_{periphery}V_{periphery} + C_{blood,gills}V_{blood,gills} + C_{blood,periphery}V_{blood,periphery}\right)/V_{body}}{C_{W,in}} \quad (5)$$

### Input data required for model application

By default, a 10 g rainbow trout with 5% body fat at 15 °C was modelled. For application of the developed models, physiological data (*e.g.* blood flow rates, ventilation rate, composition of gill tissue, blood and the rest of the organism) are required. The used parameter values are described in ESI Section 3.†

Furthermore, partition coefficients for chemical partitioning into gills, periphery and within blood are required. We here use simple approaches based on the octanol–water partition coefficient $K_{OW}$ for estimation of these partition coefficients because it generates a better general intuitive understanding about how hydrophobicity affects the outcome of the model results. We note that a more precise way for estimating tissue partition coefficients is based on the pp-LFER approach[31] but this approach is only applicable to cases of actual chemicals and, by that, not suitable for a generic analysis. The partition coefficients for the different tissues are calculated based on log $K_{OW}$ analogous to the approach from Saunders *et al.*:[32]

$$K_{tissue/water} = lipid_{tissue} \times K_{OW} + protein_{tissue} \times 0.05 \times K_{OW} + water_{tissue} \quad (6)$$

In this equation, $protein_{tissue}$ is the protein content of the tissue of interest (as volume fraction mL mL$^{-1}$), $lipid_{tissue}$ is the lipid content of the tissue of interest (as volume fraction) and $water_{tissue}$ the water content of the tissue of interest (composition data is presented in ESI Section 3†).

The uptake kinetics of chemicals from the respiration water into the blood was estimated *via* their respective permeabilities. It was assumed that a barrier consisting of aqueous boundary layers (ABL), mucus, cell membranes and cytosol must be overcome for uptake into the blood. Separate permeabilities were calculated for each of the individual layers of this barrier, which were then used to estimate the total permeability ($P_{gills}$) in the gills. A detailed description of the used parameters values and equations for estimating the permeability is also provided in ESI Section 3.†

## Results & discussion

### Experimental dataset on sorption kinetics in plasma

The desorption experiments yield concentration–time profiles showing the test chemical concentration after passage through the capillary relative to the initial concentration. These concentration–time profiles result from the chemical being extracted from the plasma solution into the PDMS as soon as the chemical desorbs from the binding components of plasma during passage through the capillary. By this, the concentration–time profiles allow the determination of desorption rate constants *via* fitting. As an example the data for extraction of 1,8-dibromooctane from 25× and 100× fold diluted plasma is shown in Fig. 2. Plotted are average values of duplicates and standard deviations are indicated as error bars. Fig. 2 shows that for both plasma dilutions the concentration of 1,8-dibromooctane was almost zero after 30 s or 60 s residence time inside the capillary, respectively. The generated data were modeled with the developed transport model and a desorption rate constant of 0.2 s$^{-1}$ was determined.

The determined desorption rate constants for all tested chemicals are summarized in Table 1. The corresponding sorption rate constants can be determined from the equilibrium constant and the determined desorption rate constant without the need for further experiments (see ESI Section 4†) and are also included in Table 1.

All determined desorption rate constants are in a range of 0.1 s$^{-1}$ to 0.4 s$^{-1}$. By that, the here determined desorption rate constants are at the lower end of the range of desorption rate constants measured with the same method for bovine albumin (0.2–1.8 s$^{-1}$).[19] The desorption rate constants for albumin varied up to one order of magnitude and were directly related to molecular weight of the chemicals: the desorption rate constants for rainbow trout plasma constituents seem to be located within a narrow range without any clear correlation to molecular properties of the sorbing chemicals. The reason for this could be the following: different from the situation with albumin, the sorbing components in plasma are not a homogeneous sorption phase but a mixture of different proteins and lipoproteins. Accordingly, the different sorption processes

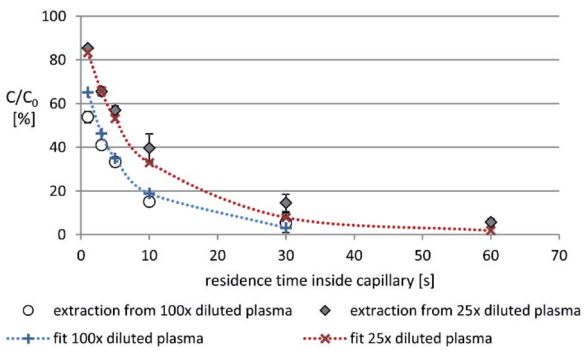


Fig. 2 Extraction of 1,8-dibromooctane from plasma. Different plasma dilutions are indicated as diamonds (25× dilution) and dots (100× dilution). Shown are mean values of duplicates, standard deviations are indicated as error bars. In cases where error bars are invisible, they are covered by the symbols. Corresponding fits with desorption rate constants $k_{des}$ = 0.2 s$^{-1}$ are indicated as crosses with interpolated lines between the calculated data points.

could have different kinetics. In the used data analysis procedure, however, these different sorption processes are not resolved but a single joint kinetics is fitted because resolution of all involved sorption processes is not feasible.

### Modeled impacts of sorption kinetics in blood on uptake, elimination and BCF

We calculated the uptake efficiency, elimination efficiency and the BCF with the model considering sorption kinetics in blood for varying sorption rate constants. The evaluated range of sorption rate constants was not limited to the experimentally determined values, but a much greater theoretical range was evaluated to elaborate general effects. Furthermore, we represent different scenarios in terms of chemical hydrophobicity and elimination *via* biotransformation kinetics by varying assumed $\log K_{OW}$ and biotransformation rate constants (biotransformation is assumed to occur only in the periphery, not in gills or blood). The purpose of these simulations is to gain a basic mechanistic understanding of the underlying processes. These simulations represent various general scenarios and are not substance-specific calculations, we thus do not provide conclusions on model uncertainty for specific chemicals.

In Fig. 3, we exemplarily show the modeled effects of slow sorption kinetics for a scenario of a chemical with a $\log K_{OW} = 6$ and a whole-body elimination rate constant $k_2$ of 4 $d^{-1}$. This whole-body elimination rate constant was estimated from an *in vitro* biotransformation rate constant of 10 $h^{-1}$ using a recently published *in vitro–in vivo* extrapolation tool.[1] Given the typical range of *in vitro* biotransformation rate constants,[33] a value of 10 $h^{-1}$ already represents a scenario of fast biotransformation. Thus, limitations are already more likely for this scenario than for other scenarios with slower elimination, because limitations by slow binding kinetics become strongest when the other kinetic processes are fast compared to the binding kinetics.

Fig. 3 shows that for sorption rate constants higher than 10 000 $L_W\ L_{sorbcomp}^{-1}\ s^{-1}$ there are no effects on uptake and elimination efficiency and thus neither on the BCF. In a range of sorption rate constants between 10 000 $L_W\ L_{sorbcomp}^{-1}\ s^{-1}$ and 100 $L_W\ L_{sorbcomp}^{-1}\ s^{-1}$, a strong decrease in elimination efficiency is observed (by one order of magnitude). The reason for this is that slow binding kinetics limit the delivery of the chemical into the eliminating tissues in the periphery of the organism, because bound chemical must first desorb into the freely dissolved state before it can permeate into the eliminating tissues. A decreased elimination can lead to higher BCF values because the chemical is less efficiently cleared. Fig. 3, however, shows that the BCF changes only slightly (from ≈70 to ≈150 L $kg^{-1}$) for this range of sorption rate constants. The uptake efficiency remains nearly unchanged in the range of sorption rate constants between 10 000 $L_W\ L_{sorbcomp}^{-1}\ s^{-1}$ and 100 $L_W\ L_{sorbcomp}^{-1}\ s^{-1}$.

For sorption rate constants smaller than 100 $L_W\ L_{sorbcomp}^{-1}\ s^{-1}$, the elimination efficiency declines further. In addition, there are now also effects on uptake efficiency and BCF: the uptake efficiency shows a decrease from ≈0.8 to ≈0.2 for slower sorption rate constants, while the BCF increases up to ≈1500 L $kg^{-1}$ for slower sorption kinetics. The uptake efficiency of the chemical decreases because the onward transport of the chemical into the rest of the body is limited when sorption of the chemical to the binding components of blood (lipids, proteins) is slow. The chemical then accumulates in the gill tissue which leads to a decreasing chemical gradient between gill tissue and ventilated water and thus the uptake efficiency reduces. The fact that the increase in BCF occurs simultaneously to the decrease in uptake efficiency does not seem plausible at first, because one would expect that a lower uptake leads to decreased BCF values. The steady-state concentration

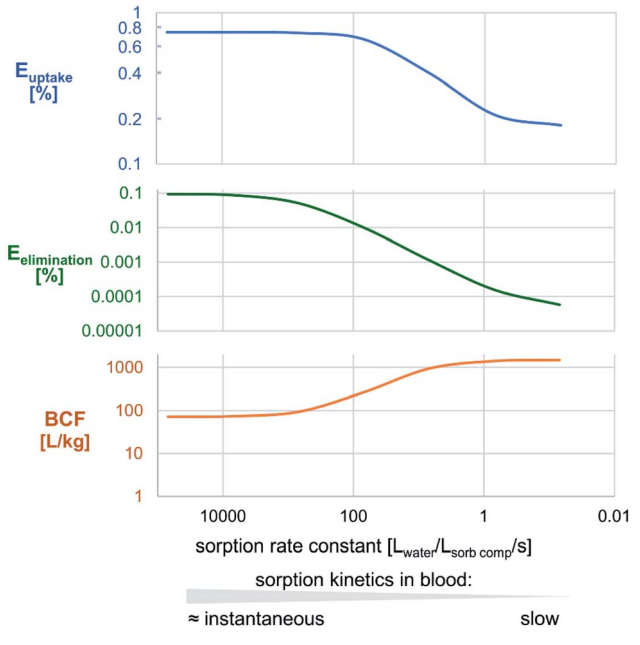


Fig. 3 Change in uptake efficiency ($E_{uptake}$), elimination efficiency ($E_{elimination}$) and bioconcentration factor (BCF) for a scenario of a chemical with a $\log K_{OW} = 6$ and a whole-body elimination rate constant of 4 $d^{-1}$ depending on the sorption kinetics in blood.

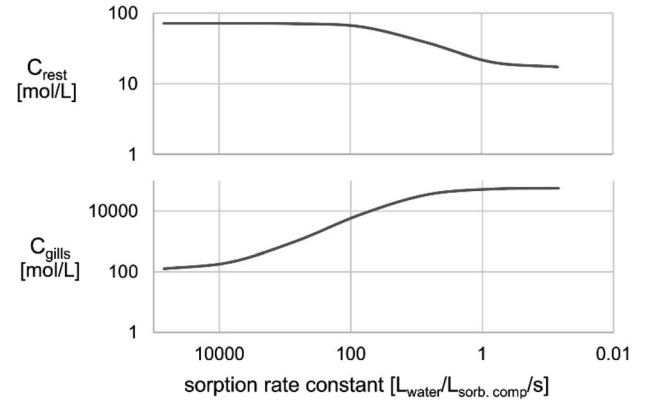


Fig. 4 Change in the steady-state concentrations in gills and rest body ($C_{gills}$ and $C_{rest}$) for a scenario of a chemical with a $\log K_{OW} = 6$ and a whole-body elimination rate constant of 4 $d^{-1}$ depending on sorption kinetics in blood.

 

in the rest of the body $C_{rest}$ (Fig. 4) does indeed show that $C_{rest}$ decreases as soon as the uptake efficiency decreases, so there is less chemical in the rest body. The steady-state concentration in the gills ($C_{gills}$), however, shows a strong increase as soon as the uptake efficiency decreases indicating that the chemical accumulates strongly in the gills (Fig. 4). The resulting concentration increase in the gills is so extreme that it causes the observed increase of the BCF. Note that if (contrary to what is assumed here) significant biotransformation occurred in the gills, such an increase in concentration would not be observed in the gills.

Apart from the potential implications for bioaccumulation, the above results could also be of relevance for toxicity assessments, *in vitro–in vivo* extrapolation of toxicity information or exposure modelling. Fig. 4 shows that for slow sorption kinetics the chemical concentration in the gills increases dramatically. A model neglecting sorption kinetics could not predict these high chemical concentrations in gill tissue. Accordingly, neglecting sorption kinetics could erroneously lead to the indication that the concentration is not high enough to cause toxic effects while in fact the concentration could be far above the threshold for toxicity in specific organs.

The effects described above also occur in scenarios with other elimination rate constants, but the numerical values are shifted. For example, in case one arbitrarily assumes a tenfold slower whole-body elimination rate constant of 0.4 $d^{-1}$ (data shown in ESI Section 5†), there still is a decrease in elimination and uptake efficiency for slower sorption rate constant leading to increasing BCF values. However, while for the above example with a whole-body elimination rate constant of 4 $d^{-1}$ $E_{elimination}$ decreases up to 3 orders of magnitude and the BCF increases by more than one order of magnitude for slow sorption rate constants, the effects are smaller for a scenario with a whole-body elimination rate constant of 0.4 $d^{-1}$: $E_{elimination}$ reduces up to two orders of magnitude and the BCF increases only by factor 2–3 (Table 2). The reason for these observations is the fact that a potential limitation due to slow binding kinetics in blood becomes most relevant when subsequent processes (*e.g.* elimination) are fast compared to the binding kinetics.

For scenarios with log $K_{OW}$ values other than 6 analogous effects can be observed, however, the impact of sorption kinetics decreases with decreasing log $K_{OW}$. Less hydrophobic chemicals have a lower tendency to bind to blood components and thus the impact of sorption kinetics also becomes less important. Fig. 5 illustrates the relation between sorption rate constant, partition coefficient and either uptake efficiency (Fig. 5 upper panel) or BCF (Fig. 5 lower panel), respectively.

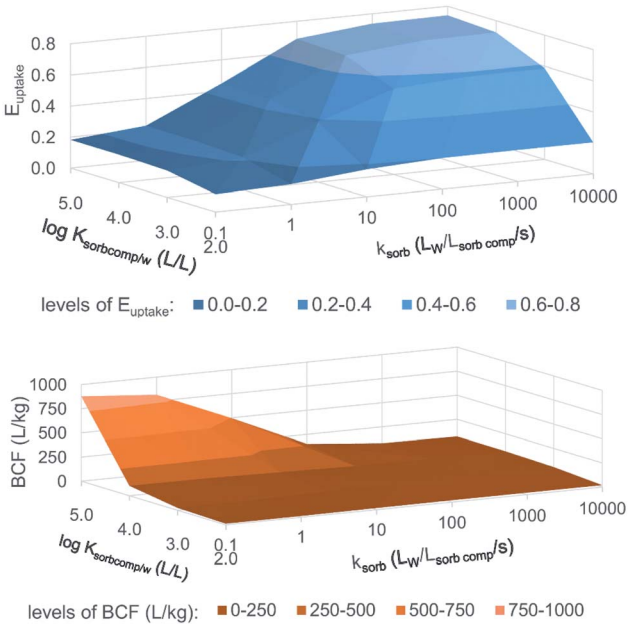


Fig. 5 Calculation of the uptake efficiency ($E_{uptake}$) and bioconcentration factor (BCF) in dependency of the partition coefficient between sorbing plasma components and water $K_{sorbcomp/w}$ (L $L^{-1}$) and the sorption rate constant $k_{sorb}$ ($L_W$ $L_{sorbcomp}^{-1}$ $s^{-1}$).

Fig. 5 shows that the less hydrophobic a chemical is, the smaller is the impact of sorption kinetics on uptake efficiency and BCF: for a chemical with a log $K_{sorbingcomonents/water} = 5$ $L_W$ $L_{sorbcomp}^{-1}$, the uptake efficiency reduces from ≈0.8 to ≈0.2 for the here evaluated range of $k_{sorb}$, while the uptake efficiency for a chemical with log $K_{sorbingcomonents/water} = 2$ $L_W$ $L_{sorbcomp}^{-1}$ changes only slightly from ≈0.2 to ≈0.1 for the same range of $k_{sorb}$. The same can be observed for the BCF; the BCF for a chemical with a log $K_{sorbingcomponents/water} = 5$ changes notably for the evaluated $k_{sorb}$ range while the BCF for a chemical with a log $K_{sorbingcomponents/water} = 2$ remains nearly constant. The explanation for this observation is that for less hydrophobic chemicals only a small proportion of chemical in the blood actually binds to the sorbing components and thus the sorption kinetics cannot have a great influence. The corresponding graph for elimination efficiency shows analogous effects and can be found in ESI Section 6.†

Considering both, the determined sorption rate constants and the sorbing plasma components–water partition coefficients, one now can evaluate whether a significant limitation of uptake or elimination due to sorption kinetics is to be expected

Table 2 Change of elimination efficiency ($E_{elimination}$) and bioconcentration factor (BCF) for slow sorption rate constants depending on the assumed whole-body elimination rate constants

| | Whole-body elimination rate constant | |
|---|---|---|
| Resulting effect | 4 $d^{-1}$ | 0.4 $d^{-1}$ |
| Reduction of $E_{elimination}$ | Up to 3 orders of magnitude (from 0.1 to 0.0001) | Up to 2 orders of magnitude (from 0.01 to 0.0001) |
| Increase of BCF | >One order of magnitude (from 70 L $kg^{-1}$ to 1500 L $kg^{-1}$) | By factor 2–3 (from 700 L $kg^{-1}$ to 1600 L $kg^{-1}$) |

for the above test chemicals. The slowest sorption rate constants were derived for *n*-propylbenzene, di-*n*-pentylether and 1,2,4-trichlorobenzene (Table 1). At the same time, however, the sorbing blood components–water partition coefficients for these chemicals are in the low range ($\log K = 2$–3, Table 1), so that for none of the test chemicals a significant limitation of uptake or elimination due to sorption kinetics is to be expected (Fig. 5). Considering all relevant factors, *i.e.* the sorption rate constant, the sorbing blood components-water partition coefficient and the biotransformation kinetics, it can be concluded from the modeling results that for most chemicals significant limitations due to slow binding kinetics appear unlikely.

## Conclusion

The derived experimental dataset on binding kinetics in plasma shows that the sorption rate constants for the investigated test chemicals are fast enough to prevent any limitations. The generic modeling analysis further indicates that this result seems to be valid for most chemicals. Only for extreme parameter combinations in terms of chemical hydrophobicity and assumed rate constants for plasma binding, respiratory uptake of chemicals is limited due to slow binding kinetics. In these cases, the chemical then accumulates in the gills leading to increasing BCF values.

In general, however, limitation of uptake or other modeling related aspects (*e.g.* consideration of the potential first-pass effects in fish gills[1]) seem to be unlikely explanations for potential discrepancies between experimental and predicted BCF. In our opinion, it is more likely that explanations for such discrepancies could lie on the part of the *in vitro* methods used to determine biotransformation kinetics. For example, one particularly relevant aspect could be enzyme induction: induction of biotransformation enzymes in the living animal over the duration of a BCF study is a factor that cannot be represented in *in vitro* assays lasting only a few hours. If significant enzyme induction occurs *in vivo*, the *in vitro* assays would underestimate the actual biotransformation and predictions using this biotransformation information would thus overestimate bioaccumulation.

## Conflicts of interest

There are no conflicts to declare.

## Acknowledgements

We thank Markus Brinkmann for provision of rainbow trout plasma and Nina Klötzer for helpful lab assistance. This research was financially supported by the German Environment Agency under FKZ 3718 65 406 0 and by CEFIC LRI (ECO 47 project).

## References

1 S. Krause and K.-U. Goss, Comparison of a simple and a complex model for BCF prediction using *in vitro* biotransformation data, *Chemosphere*, 2020, **256**, 127048.
2 J. J. Trowell, F. A. P. C. Gobas, M. M. Moore and C. J. Kennedy, Estimating the Bioconcentration Factors of Hydrophobic Organic Compounds from Biotransformation Rates Using Rainbow Trout Hepatocytes, *Arch. Environ. Contam. Toxicol.*, 2018, **75**, 295–305.
3 J. W. Nichols, D. B. Huggett, J. A. Arnot, P. N. Fitzsimmons and C. E. Cowan-Ellsberry, Toward improved models for predicting bioconcentration of well-metabolized compounds by rainbow trout using measured rates of *in vitro* intrinsic clearance, *Environ. Toxicol. Chem.*, 2013, **32**, 1611–1622.
4 J. A. Arnot and F. A. P. C. Gobas, A Generic QSAR for Assessing the Bioaccumulation Potential of Organic Chemicals in Aquatic Food Webs, *QSAR Comb. Sci.*, 2003, **22**, 337–345.
5 J. A. Arnot and F. A. P. C. Gobas, A food web bioaccumulation model for organic chemicals in aquatic ecosystems, *Environ. Toxicol. Chem.*, 2004, **23**, 2343–2355.
6 OECD, *Test No. 319A: Determination of in vitro intrinsic clearance using cryopreserved rainbow trout hepatocytes (RT-HEP)*, 2018.
7 OECD, *Test No. 319B: Determination of in vitro intrinsic clearance using rainbow trout liver S9 sub-cellular fraction (RT-S9)*, 2018.
8 D. N. Brooke, M. J. Crookes and D. A. S. Merckel, Methods for predicting the rate constant for uptake of organic chemicals from water by fish, *Environ. Toxicol. Chem.*, 2012, **31**, 2465–2471.
9 J. Chen, J. E. Schiel and D. S. Hage, Noncompetitive peak decay analysis of drug–protein dissociation by high-performance affinity chromatography, *J. Sep. Sci.*, 2009, **32**, 1632–1641.
10 M. J. Yoo and D. S. Hage, Use of peak decay analysis and affinity microcolumns containing silica monoliths for rapid determination of drug–protein dissociation rates, *J. Chromatogr. A*, 2011, **1218**, 2072–2078.
11 X. Zheng, Z. Li, M. I. Podariu and D. S. Hage, Determination of rate constants and equilibrium constants for solution-phase drug–protein interactions by ultrafast affinity extraction, *Anal. Chem.*, 2014, **86**, 6454–6460.
12 P. Li, Y. Fan, Y. Wang, Y. Lu and Z. Yin, Characterization of plasma protein binding dissociation with online SPE-HPLC, *Sci. Rep.*, 2015, **5**, 14866.
13 R. A. Weisiger, Dissociation from albumin: a potentially rate-limiting step in the clearance of substances by the liver, *Proc. Natl. Acad. Sci. U. S. A.*, 1985, **82**, 1563–1567.
14 L. M. Berezhkovskiy, Determination of hepatic clearance with the account of drug-protein binding kinetics, *J. Pharm. Sci.*, 2012, **101**, 3936–3945.

 

15 L. M. Berezhkovskiy, Some features of the kinetics and equilibrium of drug binding to plasma proteins, *Expert Opin. Drug Metab. Toxicol.*, 2008, **4**, 1479–1498.
16 S. Krause and K.-U. Goss, The impact of desorption kinetics from albumin on hepatic extraction efficiency and hepatic clearance: a model study, *Arch. Toxicol.*, 2018, **92**, 2175–2182.
17 J. A. Jansen, Influence of plasma protein binding kinetics on hepatic clearance assessed from a "tube" model and a "well-stirred" model, *J. Pharmacokinet. Biopharm.*, 1981, **9**, 15–26.
18 M. Yoon, H. J. Clewell 3rd and M. E. Andersen, Deriving an explicit hepatic clearance equation accounting for plasma protein binding and hepatocellular uptake, *Toxicol. In Vitro*, 2013, **27**, 11–15.
19 S. Krause, N. Ulrich and K.-U. Goss, Desorption kinetics of organic chemicals from albumin, *Arch. Toxicol.*, 2018, **92**, 1065–1074.
20 B. I. Escher, C. E. Cowan-Ellsberry, S. Dyer, M. R. Embry, S. Erhardt, M. Halder, J. H. Kwon, K. Johanning, M. T. Oosterwijk, S. Rutishauser, H. Segner and J. Nichols, Protein and lipid binding parameters in rainbow trout (*Oncorhynchus mykiss*) blood and liver fractions to extrapolate from an *in vitro* metabolic degradation assay to *in vivo* bioaccumulation potential of hydrophobic organic chemicals, *Chem. Res. Toxicol.*, 2011, **24**, 1134–1143.
21 P. Poulin, F. J. Burczynski and S. Haddad, The Role of Extracellular Binding Proteins in the Cellular Uptake of Drugs: Impact on Quantitative In Vitro-to-In Vivo Extrapolations of Toxicity and Efficacy in Physiologically Based Pharmacokinetic-Pharmacodynamic Research, *J. Pharm. Sci.*, 2016, **105**, 497–508.
22 J.-H. Kwon, H.-J. Lee and B. I. Escher, Bioavailability of hydrophobic organic chemicals on an *in vitro* metabolic transformation using rat liver S9 fraction, *Toxicol. in Vitro*, 2020, **66**, 104835.
23 H. Laue, L. Hostettler, R. Badertscher, K. Jenner, G. Sanders, J. Arnot and A. Natsch, Examining Uncertainty in *in Vitro-in Vivo* Extrapolation Applied in Fish Bioconcentration Models, *Environ. Sci. Technol.*, 2020, **54**, 9483–9494.
24 M. Bteich, P. Poulin and S. Haddad, The potential protein-mediated hepatic uptake: discussion on the molecular interactions between albumin and the hepatocyte cell surface and their implications for the in vitro-to-in vivo extrapolations of hepatic clearance of drugs, *Expert Opin. Drug Metab. Toxicol.*, 2019, **15**, 633–658.
25 N. I. Kramer, J. C. H. van Eijkeren and J. L. M. Hermens, Influence of albumin on sorption kinetics in solid-phase microextraction: consequences for chemical analyses and uptake processes, *Anal. Chem.*, 2007, **79**, 6941–6948.
26 P. Mayer, M. M. Fernqvist, P. S. Christensen, U. Karlson and S. Trapp, Enhanced Diffusion of Polycyclic Aromatic Hydrocarbons in Artificial and Natural Aqueous Solutions, *Environ. Sci. Technol.*, 2007, **41**, 6148–6155.
27 T. L. ter Laak, J. C. H. van Eijkeren, F. J. M. Busser, H. P. van Leeuwen and J. L. M. Hermens, Facilitated Transport of Polychlorinated Biphenyls and Polybrominated Diphenyl Ethers by Dissolved Organic Matter, *Environ. Sci. Technol.*, 2009, **43**, 1379–1385.
28 P. Mayer, U. Karlson, P. S. Christensen, A. R. Johnsen and S. Trapp, Quantifying the Effect of Medium Composition on the Diffusive Mass Transfer of Hydrophobic Organic Chemicals through Unstirred Boundary Layers, *Environ. Sci. Technol.*, 2005, **39**, 6123–6129.
29 S. Krause and K.-U. Goss, In Vitro–in Vivo Extrapolation of Hepatic Metabolism for Different Scenarios-a Toolbox, *Chem. Res. Toxicol.*, 2018, **31**, 1195–1202.
30 H. Laue, H. Gfeller, K. J. Jenner, J. W. Nichols, S. Kern and A. Natsch, Predicting the bioconcentration of fragrance ingredients by rainbow trout using measured rates of *in vitro* intrinsic clearance, *Environ. Sci. Technol.*, 2014, **48**, 9486–9495.
31 S. Endo, T. N. Brown and K.-U. Goss, General model for estimating partition coefficients to organisms and their tissues using the biological compositions and polyparameter linear free energy relationships, *Environ. Sci. Technol.*, 2013, **47**, 6630–6639.
32 L. J. Saunders, G. Diaz-Blanco, Y.-S. Lee, S. V. Otton and F. A. P. C. Gobas, Hepatic Clearance Binding Terms of Hydrophobic Organic Chemicals in Rainbow Trout: Application of a Streamlined Sorbent-Phase Dosing Method, *Environ. Sci. Technol. Lett.*, 2020, **7**, 672–676.
33 M. Halder, A. Lostia and A. Kienzler, EURL ECVAM Fish *In Vitro* Intrinsic Clearance Database, 2018.